

Enhanced photovoltage in perovskite-type artificial superlattices on Si substrates

Na Zhou^{1,2}, Kun Zhao^{1,2,3,4}, Hao Liu², Hui Bin Lu¹, Meng He¹,
Songqing Zhao², Wenxiu Leng², Aijun Wang², Yanhong Huang¹,
Kui-juan Jin¹, Yueliang Zhou¹ and Guozhen Yang¹

¹ Beijing National Laboratory for Condensed Matter Physics, Institute of Physics, Chinese Academy of Sciences, Beijing 100080, People's Republic of China

² Department of Mathematics and Physics, China University of Petroleum, Beijing 102249, People's Republic of China

³ International Center for Materials Physics, Chinese Academy of Sciences, Shenyang 110016, People's Republic of China

E-mail: zhk@cup.edu.cn (Kun Zhao) and hblu@aphy.iphy.ac.cn (Hui Bin Lu)

Received 28 April 2008, in final form 11 June 2008

Published 17 July 2008

Online at stacks.iop.org/JPhysD/41/155414

Abstract

We have fabricated a three-component perovskite-type superlattice (SL) consisting of $\text{La}_{0.9}\text{Sr}_{0.1}\text{MnO}_3$, SrTiO_3 and LaAlO_3 with atomic scale control by laser molecular beam epitaxy on Si substrates. When a He–Ne laser irradiated the superlattice by side illumination, a stable photovoltage was produced and the responsivity reached 46.7 mV mW^{-1} which is six times higher than that of a similarly grown $\text{La}_{0.9}\text{Sr}_{0.1}\text{MnO}_3$ single layer on Si substrates. This work demonstrates the potential of the present SL in photo-detectors operating at room temperature.

(Some figures in this article are in colour only in the electronic version)

1. Introduction

Perovskite-type metal oxides (PMOs) have attracted much attention for their remarkable physics properties such as piezoelectricity, ferroelectricity, ferromagnetism, superconductivity and dielectric property. The fabrication of artificial crystalline materials through layer-by-layer epitaxial growth with full control over the composition and structure at the atomic level has become one of the most exciting areas of research in condensed matter physics and material sciences. Considerable attention has recently been focused on studying enhanced functionalities of artificial PMO superlattices (SLs), for example, strong polarization enhancement [1], anomalous Hall effect [2], interface dominated biferroic nature [3], improved ferroelectricity in connection to enhanced epitaxial strain and electrostatic interaction [4] and magnetoelectric coupling at the interfaces [5]. The optical properties of PMO SLs have remained relatively unexplored, although there is

some experimental data concerning the subject of PMO p–n junctions [6–11].

In this paper, we have assembled three-component PMO SLs with different building blocks of $\text{La}_{0.9}\text{Sr}_{0.1}\text{MnO}_3$ (LSMO), SrTiO_3 (STO) and LaAlO_3 (LAO) on Si substrates with atomic scale control by laser molecular beam epitaxy (LMBE). In this SL structure, LSMO (0.387 nm) has a lattice mismatch of 2.07% with LAO (0.379 nm) and –0.9% with STO (0.3905 nm). Therefore, the LSMO layer at the LSMO/LAO interface is expected to be in compressive strain and at the LSMO/STO interface a tensile one. Thus, unusual properties induced by the interfacial effect should be expected. Previously, the SLs were fabricated on (0 0 1) $\text{SrNb}_{0.01}\text{Ti}_{0.09}\text{O}_3$ substrates, and large positive low-field magnetoresistances of 15% at 300 K and 22% at 325 K under a field of 300 Oe were observed, which was discussed in connection to the interfacial effect [12]. In this work, we have focused on the enhancement of photovoltaic characteristics of SLs under laser illuminations at room temperature compared with that of a similarly grown LSMO single layer on Si substrates.

⁴ Author to whom any correspondence should be addressed.

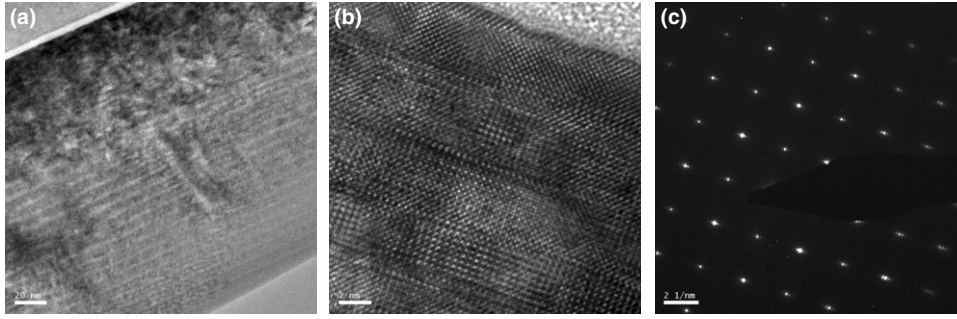


Figure 1. (a) Low magnification cross-sectional TEM image and (b) cross-sectional high-resolution TEM lattice image with (c) the corresponding SAED pattern of a SL of [LSMO/LAO/LSMO/STO]₃₀ grown on the Si substrate.

2. Experimental procedure

SLs of [LSMO/LAO/LSMO/STO]₃₀ were prepared on n-type Si (100) substrates by LMBE equipped with an *in situ* reflection high-energy electron diffraction (RHEED) system [13]. The deposition was performed at 620 °C and 2×10^{-4} Pa of oxygen pressure. The thickness of each layer was fixed at four unit cells and the modulation period Λ was about 6 nm. To improve the interface quality, a two-step method was applied and a detailed deposition procedure can be found in our previous report [7].

After the deposition, the samples were characterized by θ - 2θ x-ray diffraction (XRD) and transmission electron microscopy (TEM). For the measurements, indium electrodes were placed on the surfaces of the SL and the substrate, respectively. The photoelectric properties were investigated by using a 632.8 nm He-Ne laser with a power density of 1 mW mm^{-2} , and the signals were recorded by a 300 MHz digital oscilloscope with an input impedance of $1 \text{ M}\Omega$. The current-to-voltage curves were measured using a pulse-modulated current source under He-Ne laser illumination and in the dark. To improve the responsivity of SLs, the SL/substrate interface is illuminated directly (side illumination) as reported in our previous work [11].

3. Results and discussion

Figure 1(a) displays a low magnification cross-sectional TEM image of a SL of [LSMO/LAO/LSMO/STO]₃₀/Si after mechanical polishing and Ar ion milling. Every interface is clear and smooth. The cross-sectional high-resolution TEM image (figure 1(b)) shows a sharp interface within less than 1 nm. Although an amorphous interfacial layer of ~ 4 nm occurred between the SL and the Si substrate, no interfacial reaction layer and deviation of crystalline orientation have been observed in the SL. The modulation period is fairly uniform and close to 6 nm, which is in agreement with that calculated from the number of RHEED oscillation. Furthermore, a selected area electron diffraction (SAED) pattern (figure 1(c)) shows that the SL is single crystalline with a perfect epitaxial growth orientation relation. These results indicated that the SLs grew through the 2D layer-by-layer growth.

The single phase structure of the [LSMO/LAO/LSMO/STO]₃₀/Si SL was further confirmed using the XRD pattern.

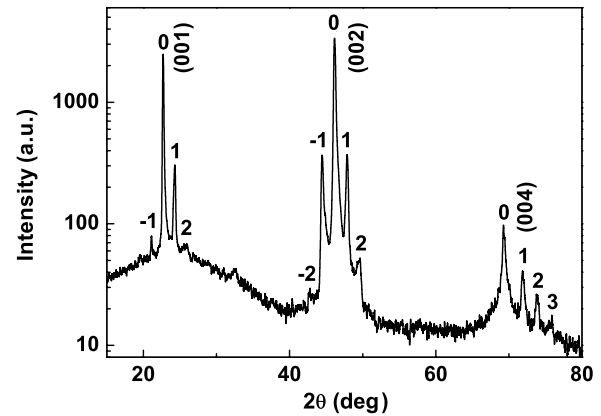


Figure 2. XRD pattern of a SL of [LSMO/LAO/LSMO/STO]₃₀ on the Si substrate. (00*l*) labels the main peak and the numbers denote the orders of the satellite peaks, confirming the long-range periodicity and high crystallinity.

As shown in figure 2, the θ - 2θ scan has no indication of the presence of additional phases other than (001) oriented layers. The higher order satellite peaks adjacent to the main peak indicated the perfect coherent heteroepitaxial growth of the LSMO, STO and LAO layers with sharp interfaces. The modulation period Λ of ~ 5.8 nm was calculated from the XRD scan using the standard formula $\Lambda = \lambda_{\text{CuK}\alpha} / (\sin \theta_{n+1} - \sin \theta_n)$, where $\lambda_{\text{CuK}\alpha}$ is the wavelength of Cu K_α radiation and n refers to the satellite peak positions.

The current-voltage characteristics of the SL were performed both in the dark and under He-Ne laser illumination at room temperature. The forward bias is defined as the current flowing from the SL to the Si substrate. As shown in figure 3, the SL exhibits good rectifying property which can be attributed to the p-n junction nature. At an applied voltage of -4 V, dark and illumination conductivities of -0.0068 mA and -0.083 mA were measured, respectively. The enhanced conductivity is in connection with the increased equilibrium carriers since the 632.8 nm photon energy is larger than the band gaps of LSMO and Si.

Figure 4 exemplifies the response of photovoltage to continuous He-Ne laser illumination measured at 300 K. The photovoltage shows a quick switch between 0 and 56 mV corresponding to the laser on and laser off. These changes occur quite reversibly and reproducibly, and no degradation was seen after switching on many times. In this case, the

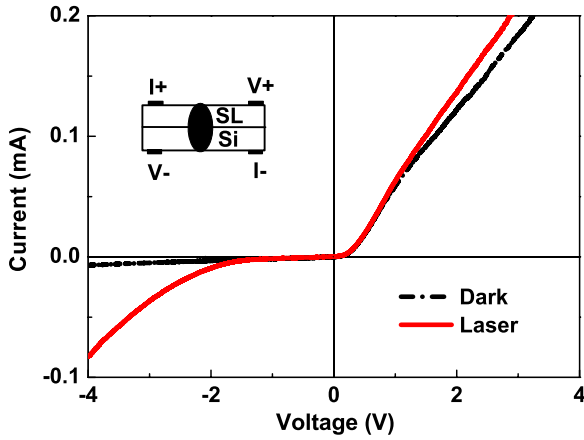


Figure 3. The current–voltage characteristics of the SL at room temperature under He–Ne laser illumination and in the dark. The inset shows a schematic illustration of the sample measurement.

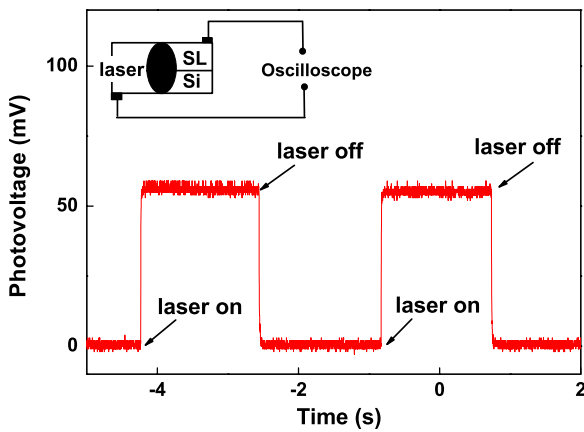


Figure 4. The steady response of a SL of [LSMO/LAO/LSMO/STO]₃₀ on the Si substrate to He–Ne laser irradiation at room temperature. The inset shows the schematic circuit of the measurement.

whole sample was ~ 0.4 mm in thickness and the diameter of the laser spot was ~ 3 mm. The effective illumination area was about ~ 1.2 mm² for the side illumination. Thus, the on-sample power was 1.2 mW. We can get a steady responsivity of 46.7 mV mW⁻¹. In addition, the spectral response of the SL as a function of the wavelength is shown in figure 5. It can be seen that the cutoff wavelengths occur at around 320 nm and 1100 nm, corresponding to the band gaps of the system.

To understand the mechanism of the photovoltaic effect of the ML, we schematically plotted the band structure as shown in figure 6. As for the He–Ne laser, the photon energy is larger than the band gaps of LSMO and Si, lower than that of STO and LAO, so the electrons and holes in LSMO and Si were created in the system. These excess carriers can be separated by the built-in potential which may be promoted by the interface-strain-induced electric fields, resulting in holes being swept into the LSMO and electrons into the Si substrate. Eventually, a photovoltage between the two electrodes occurs.

Different from the LSMO/Si p–n junction with a steady responsivity of ~ 6.87 mV mW⁻¹ [11], the present SL shows a much higher photovoltaic responsivity. As for the SL, the LSMO layer at the LSMO/LAO interface is expected to be in

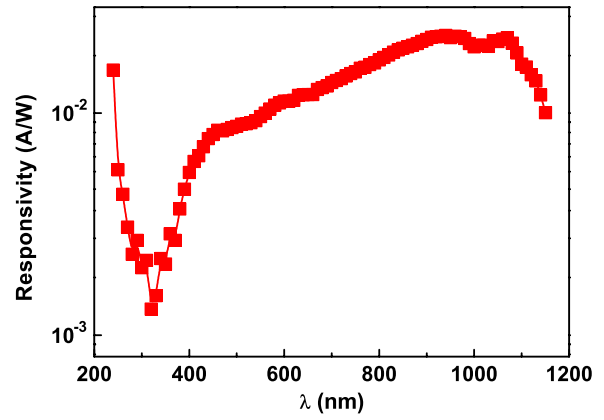


Figure 5. The spectral response of a SL of [LSMO/LAO/LSMO/STO]₃₀ on the Si substrate.

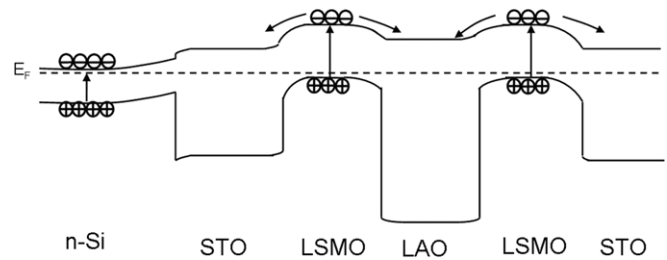


Figure 6. The schematic band structure of the [LSMO/LAO/LSMO/STO]₃₀ on the Si substrate. E_F denotes the Fermi level.

compressive strain and at the LSMO/STO interface a tensile one. Different from that induced in epitaxial single layer films due to the lattice matching to the substrate, where strains get relaxed as the thickness of the film increases, strains in the case of the SL are periodically stacked and can be kept as the thickness increases. Such an enhancement feature has not been clearly understood yet; however, we believe that it is attributed to the SL aspect involving a large number of interfaces and is probably a combined effect of finite polarization contribution coming from the STO layers [4], interface-induced ferroelectricity in the LAO layers [14], the electric charges developed at the interfaces [5] or the interface-induced strain [2].

Previously, it was suggested that interfacial strains have a tendency to create a certain randomness in the magnetic system, tending to suppress the phase separation scenario [15], and one detects order–order transitions [12, 16]. In the present case, the photovoltaic effect was studied at room temperature and without an applied magnetic field. Further experiments, such as the magnetotransmittance effect [17], illumination size dependence, polarization dependence, bias dependence and temperature dependence, are currently in progress in order to clarify the underlying detection mechanism of our three-component SL.

4. Summary

In summary, we have prepared three-component perovskite-type SLs on Si substrates by LMBE. A stable photovoltage was produced under side illumination. An increase of $\sim 600\%$

in photovoltaic responsivity has been observed in SLs over LSMO/Si p–n junctions. Our results reveal that the SL interfaces play an important role in photovoltage enhancement.

Acknowledgments

This work has been supported by the National Basic Research Program of China, the National Natural Science Foundation of China, the Key Project of the Chinese Ministry of Education and the Beijing Natural Science Foundation.

References

- [1] Lee H N, Christen H M, Chisholm M F, Rouleau C M and Lowndes D H 2005 *Nature* **433** 395
- [2] Wang L M 2006 *Phys. Rev. Lett.* **96** 077203
- [3] Chaudhuri A R, Ranjith R, Krupanidhi S B, Mangalam R V K and Sundaresan A 2007 *Appl. Phys. Lett.* **90** 122902
- [4] Bose S and Krupanidhi S B 2007 *Appl. Phys. Lett.* **90** 212902
- [5] Murugavel P, Padhan P and Prellier W 2004 *Appl. Phys. Lett.* **85** 4992
- [6] Sun J R, Xiong C M, Shen B G, Wang P Y and Weng Y X 2004 *Appl. Phys. Lett.* **84** 2611
- [7] Lu H B, Jin K J, Huang Y H, He M, Zhao K, Cheng B L, Chen Z H, Zhou Y L, Dai S Y and Yang G Z 2005 *Appl. Phys. Lett.* **86** 241915
- [8] Zhao K, Huang Y H, Zhou Q L, Jin K J, Lu H B, He M, Cheng B L, Zhou Y L, Chen Z H and Yang G Z 2005 *Appl. Phys. Lett.* **86** 221917
- [9] Huang Y H, Zhao K, Lu H B, Jin K J, Chen Z H, Zhou Y L and Yang G Z 2006 *Appl. Phys. Lett.* **88** 061919
- [10] Zhao K, Jin K J, Lu H B, Huang Y H, Zhou Q L, He M, Chen Z H, Zhou Y L and Yang G Z 2006 *Appl. Phys. Lett.* **88** 141914
- [11] Xing J, Zhao K, Liu G Z, He M, Jin K J and Lu H B 2007 *J. Phys. D: Appl. Phys.* **40** 5892
- [12] Zhao K, He M and Lu H B 2007 *Appl. Phys. Lett.* **91** 152507
- [13] Lu H B, Wang N, Chen W Z, Chen F, Zhao T, Peng H Y, Lee S T and Yang G Z 2000 *J. Cryst. Growth* **212** 173
- [14] Huang Y H, Zhao K, Lu H B, Jin K J, He M, Chen Z H, Zhou Y L and Yang G Z 2006 *Physica B* **373** 313
- [15] Baerner K 2005 *New Trends in the Characterization of CMR-Manganites and Related Materials* (Trivandrum: Research Signpost)
- [16] Feng J F, Zhao K, Zhao J G, Huang Y H, He M, Lu H B, Han X F and Zhan W S 2007 *Physica B* **387** 156
- [17] Sukhorukov Yu P, Gan'shina E A, Belevtsev B I, Loshkareva N N, Vinogradov A N, Rathnayaka K D D, Parasiris A and Naugle D G 2002 *J. Appl. Phys.* **91** 4403